IOP Conf. Series: Materials Science and Engineering **203** (2017) 012013 doi:10.1088/1757-899X/203/1/012013

# Scaling Effect on Velocity Profiles in Capillary Underfill Flow

**Fei Chong Ng**
School of Mechanical Engineering, Engineering Campus, Universiti Sains Malaysia, 14300, Nibong Tebal, Malaysia.
**Aizat Abas***
School of Mechanical Engineering, Engineering Campus, Universiti Sains Malaysia, 14300, Nibong Tebal, Malaysia.
**M Z Abdullah**
School of Mechanical Engineering, Engineering Campus, Universiti Sains Malaysia, 14300, Nibong Tebal, Malaysia.
**M H H Ishak**
School of Mechanical Engineering, Engineering Campus, Universiti Sains Malaysia, 14300, Nibong Tebal, Malaysia.
**Gean Yuen Chong**
School of Mechanical Engineering, Engineering Campus, Universiti Sains Malaysia, 14300, Nibong Tebal, Malaysia.

**Corresponding author*: aizatabas@usm.my

**Abstract.** In this paper, the scaling effect of ball grid array (BGA) device on the capillary underfill (CUF) flow and its velocity profiles is thoroughly investigated by means of fluid-structure interaction (FSI) numerical simulation. It is found that generally the flows front profiles attained from device of different scale sizes are comparable to the actual miniature BGA, with relative error approximately under 10%. Based on dimensionless number analysis, the scaling limit is estimated at 20, to maintain low scaling error. The velocity profiles attained on the CUF flow in each models of different scales are relative similar in magnitude and trend. Although the increases in gap height reduces the strength of capillary flow, the flow's velocity still be maintained and the scaling effect is counter-balance with the increases in driving pressure force. The magnitude of entrant velocity is higher at earlier stage of CUF (less than 40% filling); while higher magnitude of exit velocity is found at later stage of CUF (beyond 60% filling). Additionally, the pressure and velocity distributions of CUF flow in miniature device were also studied thoroughly.

## 1. Introduction

Capillary underfill (CUF) encapsulation is important to enhance the electronic package's reliability, cushion it from external unfavourable contamination, dissipates mechanical streets away from the solder joints as well serves as a heat sink [1, 2]. Hence, various researches were conducted in the past decades on this underfill and electronic packaging field, aimed to substantially improve and also optimize the CUF process. A cost-effective methodology is found in the underfill study, by developing the power-law constitutive equation-based analytical models to predict the underfilling flow [3]. Besides, finite volume method (FVM) simulation has been the most favourable method in simulating the CUF flow. Fluid structure interaction (FSI) scheme based on FVM numerical simulation have been incorporated in the underfill encapsulation study. Using this FSI approach, various underfill parameters has been analysed: inlet pressure, outlet vent [4], silicon chip thickness [5], solder bump arrangement and sizes [6] to optimize the CUF process. Another numerical tool known as Lattice Boltzmann method (LBM) also being

adopted to investigate the underfill process. Similar flow profiles upon side by side comparison to the FVM simulation were obtained from LBM simulation [7]. However, the LBM based software is found in certain test cases to be much costly as the computing time is generally longer than using FVM. Furthermore, various experimental study have been conducted along with numerical simulation for validation purpose. Most researches generally used a scaled-up flip chip model with a replacement fluid instead of the actual device, underfill fluid and underfilling machine [3 – 8]. This is mainly to enhance the visualization of the CUF flow across the device and also to significantly minimize the expenditure of the research work.

It had been reported that the geometrical shape and arrangement of solder bumps in flip chip are decisive factor in to the overall CUF process [9]. The CUF filling time of middle empty BGA is found to be shorter compared to the full array BGA and has less air voids occurrence [6, 8]. It is found also that the L-type dispensing method is regarded as the best option available due to its ability to yield relatively faster and uniform filling [10]. Additionally, air void and incomplete filling are rarely found when L-type dispensing method is being adopted [11]. Furthermore, the impact of varying the BGA's gap height is investigated and showed that the increase in gap height is capable of reducing the void formation as well as further promote the CUF flow [12]. The scaling effect however is not being emphasized here as only one dimension of the BGA gap height is being manipulated, instead of its width and length dimensions.

Generally, the study of FSI numerical simulation on CUF encapsulation is rather limited in number, while the scaling effect of BGA on the CUF process is scarcely investigated. To date, there is no existing numerical FSI study on the scaling effect of the CUF encapsulation of BGA device has been found that is concentrated on the velocity distributions of the CUF encapsulation process. The velocity is essentially an important parameter in deciding the flowability of the encapsulant into the gap of the BGA. Extracting velocity data from underfilling fluid is difficult to be achieved through experimental works, since sophiscasted equipment were required. Fortunately, numerical simulation like FVM able to provide data on the velocity profiles. Therefore, through this numerical study, the impact of altering the package's size by scaling on flow's velocity and dynamics can be clearly visualized. This definitely will provide an insight to package designers on relevant scaling issues, to design an optimized underfill process and BGA package.

## 2. Problem Descriptions

Fig. 1 depicts the capillary underfill (CUF) encapsulation process of BGA flip chip. Controlled amount of underfill epoxy mold (encapsulant) is dispensed at one or more side. Subsequently, the encapsulant will flow into the gap between flip-chip and substrate via capillary action. The separation between flip chip and substrate is known as the gap height. It is the parameter that defines the strength of capillary flow [8, 13].

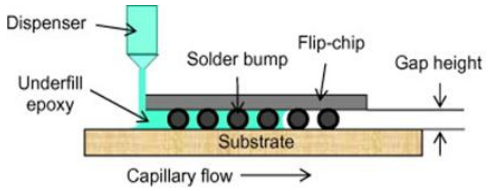


**Fig. 1.** Schematic of BGA chip underfilling boundary conditions [14].

In this study, the three-dimensional CUF flow in middle empty BGA that is subjected under L-type dispensing method is simulated numerically. Middle empty BGA is chosen due to its popularity usage in the industrial applications compared to full and perimeter orientations. Similarly, the L-type dispensing method is much more favourable in the industry as the occurrence of air void and incomplete filling are less likely compared to the U-type and I-type. Meanwhile, to account for the scaling effect, in this present paper, the CUF process of four different scaled-up BGA models were studied together with actual miniature device.

## 3. FSI Numerical Simulations

The conventional finite volume method (FVM) based software, Ansys FLUENT was used to simulate the fluid flows and its dynamic properties in the CUF encapsulation process of middle empty orientation BGA for various scale sizes under L-type dispensing method. Multiphase fluid structure interaction (FSI) was adopted to enhance the accuracy of the simulation works since it will enable precise prediction of the interactions between both fluid and structure domains. Governing equations of Navier-stokes will be discretized based on FVM scheme and solved numerically, together with VOF equation. The dimensions of the actual size BGA and scaled-up BGA models were shown in Table 1. The material properties of Sn-3.0 Ag-0.5 Cu solder bumps in BGA and underfill encapsulant are presented in Table 2.

| Scale size | Dimensions of BGA models (mm) | | | |
|---|---|---|---|---|
| | Bump diameter | Bump pitch | Gap height | Length |
| 1.0 | 0.5 | 1.0 | 0.45 | 12.5 |
| 4.4 | 2.2 | 4.4 | 2.0 | 55.0 |
| 6.0 | 3.0 | 6.0 | 2.7 | 75.0 |
| 8.0 | 4.0 | 8.0 | 3.6 | 100.0 |
| 11.0 | 5.5 | 11.0 | 5.0 | 137.5 |

**Table 1.** Dimensions of actual size BGA (scale size 1.0) and various scaled-up BGA models.

| Sn-3.0 Ag-0.5 Cu solder bump | | | Underfill encapsulant | | |
|---|---|---|---|---|---|
| Material property | Unit | Value | Material property | Unit | Value |
| Density | $g/cm^3$ | 7.04 | Density | $g/cm^3$ | 1.8 |
| Elastic modulus | GPa | 37.4 | Molecular weight | kg/kg·mol | 44.05 |
| Poisson's ratio | - | 0.34 | Viscosity | kg/m·s | 2.2 |
| | | | Surface tension | N·m | 0.06 |

**Table 2.** Material properties of solder bump and underfill encapsulant.

Path conforming tetra meshing technique is primarily used in all simulation works presented here to create high quality mesh that are properly discretized that compatible with FLUENT. Figs. 2 (*a*), (*b*) and Figs. 2 (*c*), (*d*) depicted the meshed geometry of the structural solid and fluid domains respectively.

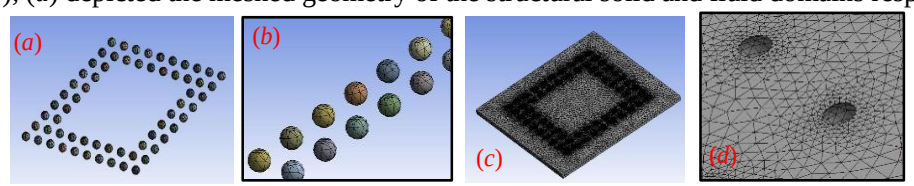


**Fig. 2.** Meshed geometry in (*a*, *b*) structural solid and (*c*, *d*) fluid domains.

All CUF encapsulation numerical simulations are set under constant temperature, $T_0$. Both initial inlet and outlet gauge pressures are set to as 0 Pa (equal to atmospheric pressure) to model the capillary flow. Generally, all initial and boundary conditions (BC) used are summarized as follow:

(*a*) **On wall**: $u = v = w = 0; \quad T = T_0; \quad \frac{\partial p}{\partial n} = 0$

(*b*) **At inlet**: $P = P_{in}(x, y, z, t); \quad T = T_0$

(*c*) **On flow front**: $P_{atm} - \frac{\sigma}{R} = P_{atm} - \frac{2\sigma cos\theta}{b}$

L-type dispensing method is modelled in the simulation by designating the sides of the inlet and outlet BC, as illustrated in Fig. 3. No-slip boundary conditions is applied on all wall surfaces and FSI regions. Wall adhesion setup is enabled to accurately predict the shape of the flow meniscus. FSI simulation is achieved by using the built-in System Coupling module that iteratively coupling the results from Transient Structural and FLUENT. Transient pressure-based solver is selected in the simulation works. Multiphase formulation is enable by specifying the two Eulerian phases that are involved in the simulation models where the air will be set as the primary phase while underfill encapsulant as the secondary phase.

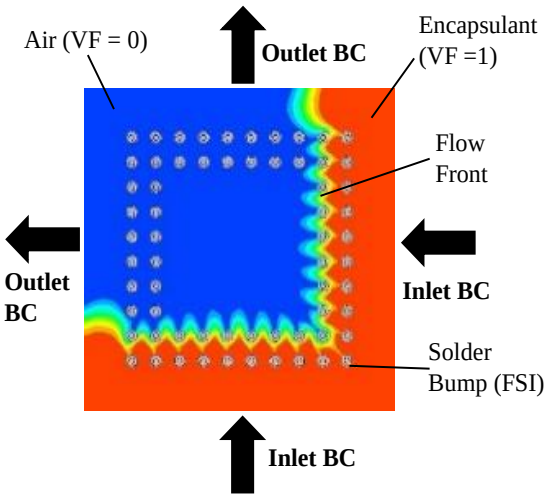


**Fig. 3.** Boundary conditions illustrated the L-type dispensing method.

## 4. Results and Discussions

### 4.1. Flow Front Comparison between Scaled-up BGA Model and Actual Size Device

All the BGA models of different scaling are compared side-by-side to the actual size BGA, in term of front advancement of the encapsulant flow at 40% filling, as shown in Fig. 4. Eventually it appears that the flow front profile of CUF flow in the actual size BGA compares well and is found to be almost similar to the profiles in the scaled-up BGA models, with approximate disparity within 10%. It is showed that scaled-up BGA models can be used to replace the actual miniature device to enhance the visualization aspects in the study of CUF flow. This validation study also compares well with that reported by Aizat et al. [8] in Fig. 5.

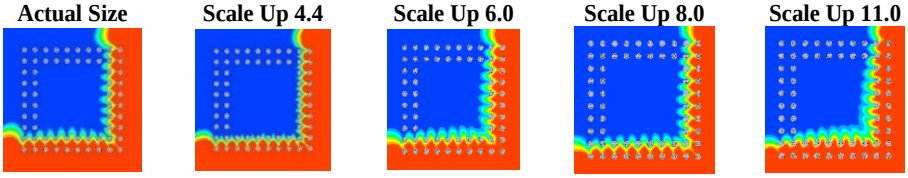

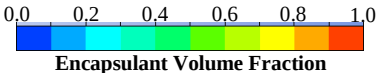


**Fig. 4.** Comparison of flow front profiles at 40% filling in actual size BGA and scaled-up BGA model.

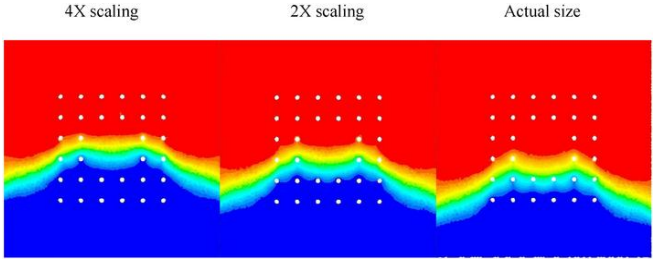


**Fig. 5.** Comparison of scaling effect and the underfill flow in actual size device based on the works of Aizat et al. [8]

## 4.2. CUF Velocity Variations near the Dispensing Inlet

In Fig. 6, the velocity of the encapsulant near the inlet for all BGA models shows a qualitatively similarly trend, with its magnitudes falling in the range of 4.0 – 5.9 mm/s, for except the highest flow velocity of 8.7879 mm/s in the actual size BGA during the 20% filling. This eventually shows that the scaling effect did not affect the kinematic of the encapsulant flow across the BGA since its velocity remains invariant. Capillary pressure reduces as the gap height increases in larger scaled up BGA model. However, the reduction in capillary pressure is compensated by the increase in the quantity of dispensed encapsulant. Consequently, this will increase the hydrostatics pressure of the encapsulant due to its weight component to further reduce the filling time. Generally, the encapsulant's velocity reaches peak value at 20% of filling as observed in the actual size BGA and all scaled-up BGA models. This is because in the beginning of CUF process, the encapsulant only flows pass few rows and experiences lowest cumulative bump's resistance. The substantial high net driving pressure is found for the case of fast encapsulant flow particularly at the onset of CUF encapsulation. Subsequently, at CUF after 40% of filling, this net pressure would reduce substantially due to the increasing cumulative solder bump resistance. This will cause the encapsulant to decelerate and having almost similar velocity thereafter until near-completion of the CUF process.

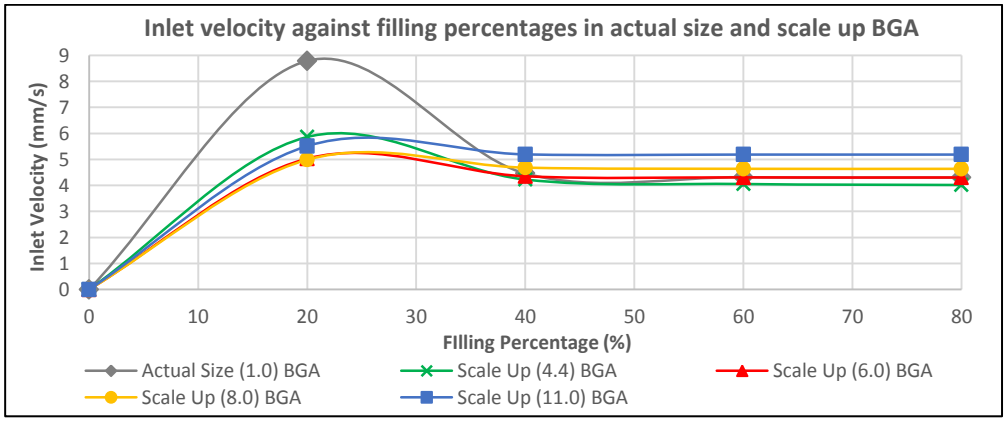


**Fig. 6.** Inlet velocity of flow at various filling percentages for actual size and scaled-up BGA models.

## 4.3. CUF Velocity Variations near the Dispensing Outlet

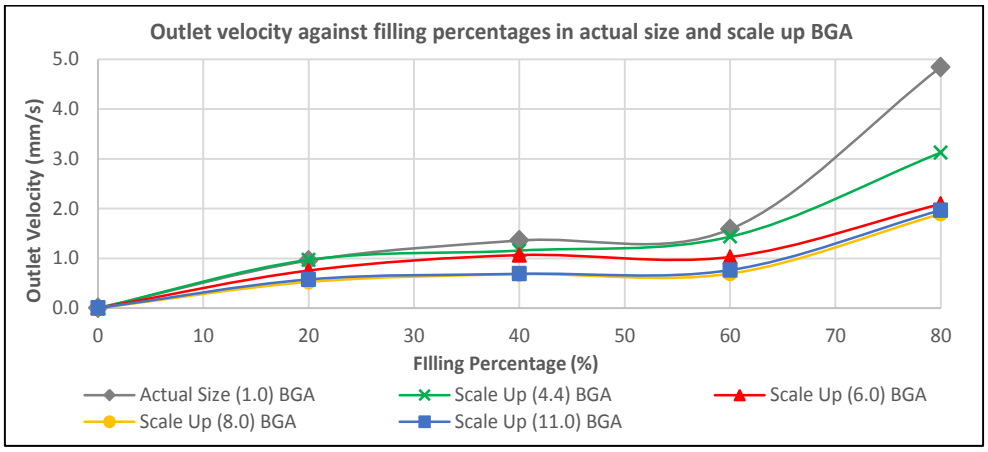


**Fig. 7.** Outlet velocity of flow at various filling percentages for actual size and scaled-up BGA models.

The velocity of the fluid flow, i.e. the displacing air, near the dispensing outlet vent at different filling percentages for both actual size and scaled-up BGA models are presented graphically in Fig. 7. Upon comparison to the magnitude of encapsulant's inlet velocity, it is found that the rate of air being displaced is slower due to limited quantity of air available in the cavity in contrast to larger quantity of encapsulant in the inlet reservoir that is subjected to the capillary pressure. Moreover, the velocity of the air near the outlet gradually increases as the encapsulant flows during the earlier CUF stages (before 60% of filling) is shown to peak drastically, with highest velocity recorded during 80% of filling. Furthermore, it appeared that the air velocity in actual size BGA is the highest compared to the scaled up BGA at all time. Meanwhile, the 6.0, 8.0 and 11.0 scaled up BGA models have fairly similar outlet vent velocity.

### 4.4. Pressure and Velocity Distributions in Actual Size Miniature BGA Device

Comparison study conducted previously has revealed that the CUF flows in the actual size BGA is shown to have significantly faster filling rate with high entrant pressure observed. To validate these results, the pressure and velocity distributions of the CUF flow in an actual size BGA are studied. Five specific points, denoted by **P1**, **P2**, **P3**, **P4** and **P5**, are designated along the diagonal region of the PCB, with the points coordinates depicted in Fig. 8. The fluid pressure and velocity variations of the fluid at different filling percentages along these five points are identified and plotted in Fig. 9 and Fig. 10 respectively.

The pressure and velocity distributions obtained in Fig. 8 and Fig. 9 are in good agreement with the results presented earlier. The pressure at **P1** increases as the encapsulant flow progress. Meanwhile the lowest pressure is recorded at **P5** throughout the whole CUF process as it is filled with air. It is noticed that the pressure at particular point will increases rapidly when the encapsulant reached there. On other hand, the fluid's velocity at all points and filling stages are almost similar, with substantially fast fluid flow being observed during 40% at points **P2** and **P3**. This is due to the convergent of flows from both dispensing inlets and the encapsulant that starts to accelerate as it advances toward the bumps-less region. Additionally, the pressure and velocity distributions in the CUF process of actual size BGA is also depicted in Table 3, at 20%, 40%, 60% and 80% fillings.

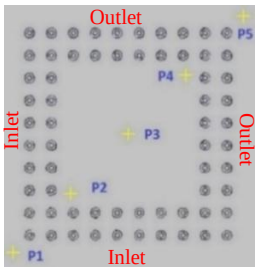


*Coordinates* (mm)
**P1**(1.3, 1.3)
**P2**(3.925, 3.925)
**P3**(6.55, 6.55)
**P4**(9.175, 9.175)
**P5**(11.8, 11.8)

**Fig. 8.** Locations of the five reference points along the diagonal of actual size BGA device.

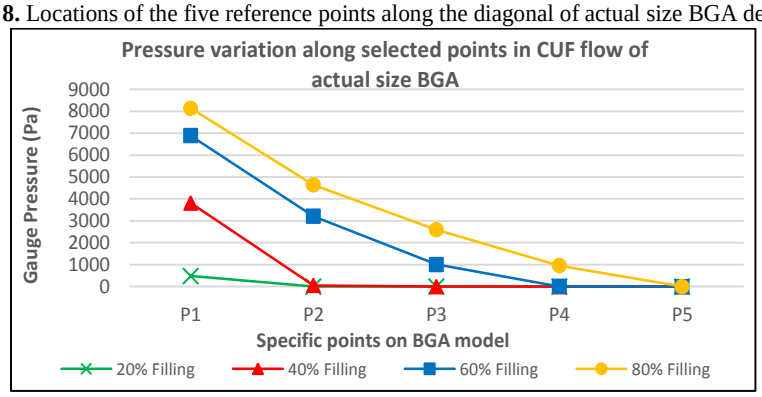


**Fig. 9.** Pressure distribution along five selected diagonal points in actual size BGA at different filling percentages.

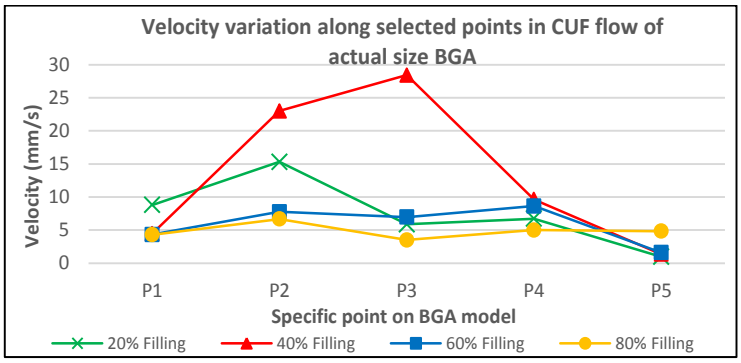


**Fig. 10.** Velocity distribution along five selected diagonal points in actual size BGA at different filling percentages.

| Filling Percentage (%) | 20 | 40 | 60 | 80 |
|---|---|---|---|---|
| 0 2 4 6 8 10 Gauge Pressure (kPa) | 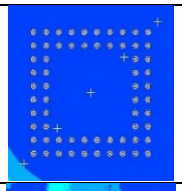 | 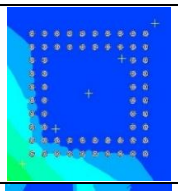 | 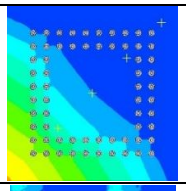 | 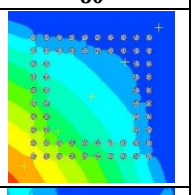 |
| 0 6 12 18 24 30 Velocity (mm/s) | 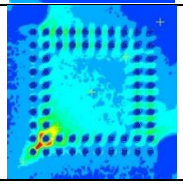 | 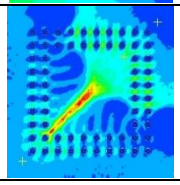 | 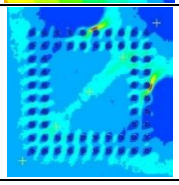 | 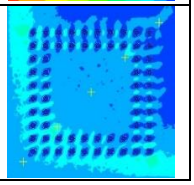 |

**Table 3.** Pressure and velocity profiles at different filling percentages for actual miniature BGA.

Generally the pressure profiles in Table 3 show the pressure is gradually building up as the encapsulant flow front progress. The incomplete fill region having zero gauge pressure will indicated that the cavity is full with air at atmospheric pressure. On the contrary, no clear different is observed between the encapsulant-filled region and unfilled (air-rich) region based on the velocity profiles in Table 3. This is because the encapsulant's velocity are almost similar. However, it is noticed that there exists a high velocity region near the diagonal line located at joining points of **P1** and **P2** respectively. This fast flowing encapsulant is due to the joining of flows from both inlets and they eventually start to accelerate due to lesser bump resistance upon entering the bump-less region. Generally the encapsulant flow has a velocity in the range of 0 – 15 mm/s indicating a steady laminar viscous flow. Furthermore, carefully analysis on the velocity profiles eventually found that the encapsulant flows much slower in the surrounding of solder bumps due to kinetic energy loss during the inelastic collision between the encapsulant and the solder bumps. As a result, the encapsulant meniscus velocity decreases gradually until the meniscus detaches from the solder bumps.

## 5. Conclusions

This paper studied the CUF encapsulant flows in the actual size miniature BGA and various scaled-up BGA models using the Fluid Structure Interaction (FSI) scheme available in commercial FVM software, ANSYS Fluent. Flow front profiles among the actual size BGA and scaled-up BGA models of various sizes are fairly similar and comparable with approximate error not exceeding 10%. This had justified the validity on the usage of scaled-up model in experimental study to enhance visualization aspect. Nevertheless, scaling effect has minimal impact on the fluid's velocity as the CUF flow possess similar inlet and outlet's velocities across all models of various sizes. The inlet's velocity is higher at earlier stage of CUF (less than 40% filling); whereas the outlet's velocity is higher toward the completion of CUF (beyond 60% filling). While the overall encapsulant flows are classified as steady viscous laminar, slower encapsulant speed is being noticed at the vicinity of the solder bumps. The pressure and velocity distributions presented for miniature BGA device illustrated clearly the variations of flow dynamics during the L-type dispensing CUF process. Essentially, these findings will served as a good foundation for future optimization works on the CUF process as well as the design of BGA chip to achieve a desirable chip's performance and reliability.

**Acknowledgements:**

This work was partly supported by the FRGS grant FRGS/1/2015/TK03/USM/03/2 and Short Term Grant 60313020 from the Division of Research and Innovation, Universiti Sains Malaysia.

**References:**

[1] H. Ardebili, M.G. Pecht, "Chapter 3 - Encapsulation Process Technology", Encapsulation Technologies for Electronic Applications, *Elsevier* (2009), pp. 129–179.
[2] Ning-Cheng Lee, "9 – BGA and CSP Assembly and Rework", *Reflow Soldering Processes* (2001), pp. 189 – 213.
[3] J.W. Wan, W.J. Zhang, D.J. Bergstrom, "Recent advances in modeling the underfill process in flip-chip packaging", *Microelectronics Journal* (2007), **38**, pp 67–75.
[4] C.Y. Khor, M.Z. Abdullah, F. Che Ani, "Study on the fluid/structure interaction at different inlet pressures in molded packaging", *Microelectronic Engineering* (2011), **88**, pp. 3182 – 3194.

[5] C.Y. Khor, M.Z. Abdullah, "Analysis of fluid/structure interaction: influence of silicon chip thickness in molded packaging, *Microelectronic Reliability* (2013), **53**, pp. 334 – 347.
[6] C.Y. Khor, M.Z. Abdullah, C.S. Lau, W.C. Leong, M.S. Abdul Aziz, "Influence of solder bump arrangements on molded IC encapsulation", *Microelectronic Reliability* (2014), **54**, pp. 796 – 807.
[7] Aizat Abas, MZ Abdullah, MHH Ishak, "Lattice Boltzmann and finite volume simulations of multiphase flow in BGA encapsulation process", *ARPN Journal of Engineering and Applied Sciences* (2015)
[8] Aizat Abas, M.S. Haslinda, M.H.H. Ishak, A.S. Nurfatin, M.Z. Abdullah, F. Che Ani, "Effect of ILU dispensing types for different solder bump arrangements on CUF encapsulation process", *Microelectronic Engineering* (2016)
[9] Y.K. Shen, T.W. Ye, S.L. Chen, C.H. Yin, W.D. Song, "Study on mold flow analysis of flip chip package", *International Communications in Heat and Mass Transfer* (2001), **28**, pp 953-952.
[10] H.R. Gwon, H.J. Lee, J.M. Kim, Y.E. Shin, S.H. Lee, "Dynamic behavior of capillary-driven encapsulation flow characteristics for different injection types in flip chip packaging", *Journal of Mechanical Science and Technology* (2014), **28 (1)**, pp 167-173.
[11] Y.K. Shen, S.T. Huang, C.J. Chen, S. Yu, "Study on flow visualization of flip chip encapsulation process for numerical simulation", *International Communication in Heat and Mass Transfer* (2006), **33**, pp 151-157.
[12] C.Y. Khor, M.Z. Abdullah, F.C. Ani, "Underfill process for two parallel plates and flip chip packaging", *International Communications in Heat and Mass Transfer* (2012), **39**, pp 1205–1212.
[13] Aizat Abas, FC Ng, MZ Abdullah, MHH Ishak, CY Chong, "CUF Scaling Effect on Contact Angle and Threshold Pressure", *to be appeared in Soldering and Surface Mount Technology*
[14] Available at "http://www.epoxysetinc.com/underfill-csp-bga/" (Assessed at 27 September 2016)